Studies of Potassium Ferrite $K_{1+x}Fe_{11}O_{17}$. III. Ionic Conductivity and Chemical Diffusion

GEOFFREY J. DUDLEY AND BRIAN C. H. STEELE

Department of Metallurgy and Materials Science, Imperial College of Science and Technology, Prince Consort Road, London, SW7, 2AZ, United Kingdom

Both the electronic and ionic conductivity of potassium ferrite ($K_{1+x}Fe_{11}O_{17}$) have been measured at 580°K as a function of x and the coupling between the two fluxes is shown to be very small. The transient behavior of voltage probes reversible to either potassium ions or electrons has been investigated and is consistent with the theory developed by Yokota (*1*) in which the transient voltages are controlled by the chemical diffusion coefficient $\tilde{D}$ of the system. The variation in ionic conductivity with x is qualitatively consistent with the predictions of Wang *et al.* (*2*) for isostructural sodium β alumina. Measurements of the entropy of dissolution of potassium in the phase strongly suggest that an ordering process is occurring at the approximate composition $K_{1.7}Fe_{11}O_{17}$.

Introduction

Alkali ferrites combine the high ionic conductivity of β alumina with a moderate electronic conductivity and wide range of nonstoichiometry, and are therefore of considerable interest as solid-solution electrode materials (*3*). Unlike in β alumina, there is the opportunity of changing the concentration of ionic (and electronic) charge carriers by means of coulometric titrations, with less danger of changing the microstructure or concentrations of other defects as is likely to happen when a series of samples with differing stoichiometry are prepared by high-temperature synthesis from different starting compositions. With their close structural resemblances to β alumina, the ferrites may also be useful model systems for studying the ionic conduction process in the former. Several measurements of diffusion, electronic conductivity, and ionic conductivity in sodium and potassium ferrites or ferrite–aluminate solid solutions, sometimes with other additives, have been reported (*4–6*) but until recently the variations as a function of stoichiometry, in particular the alkali ion

excess, had not been studied. In Part I of this study (*7*) the authors have reported measurements of the electronic conductivity of potassium ferrite as a function of the potassium excess x and as a function of temperature. In the present work the ionic conductivity and chemical diffusion coefficients have been measured also as a function of x. In addition the entropy and enthalpy of dissolution of potassium in the ferrite have been calculated from the temperature dependence of the cell emfs reported in Part I.

Experimental

Preparation of Materials

All β-alumina-type phases used were initially prepared by grinding together potassium nitrate and the trivalent metal oxide (or oxide mixture) in a mole ratio of 1:3.25 and firing at 1170°K (1370°K for potassium β alumina) for 22 hr. The resulting powders were pressed into 8 mm-diameter pellets, wrapped in platinum foil (tantalum foil for β alumina) and hot pressed in an alumina die at 1400°K for 6 hr using a pressure of 5×10^7 N m^{-2} (graphite die at 1820°K for 10 min under

1

2.7×10^7 N m^{-2} for β alumina). The resulting compacts had densities between 95 and 99% theoretical and consisted almost entirely of the two-block phase, the three-block phase being just detectable by powder diffraction. Samples were machined using an annular diamond saw and an oil lubricant.

Choice of Method for Measuring Ionic and Electronic Conductivities

Since the ratio of ionic to electronic conductivity in the ferrite was expected to vary greatly as x was changed, it was felt desirable to be able to measure both ionic and electronic conductivities independently on the same specimen. The difficulty of obtaining "nonpolarizable" potassium ion reversible electrodes for passing an ionic current through the specimen led to the use of a four-point dc technique in which a constant ionic current could be passed through the specimen between two further pieces of ferrite acting as reservoirs of potassium ions and electronically isolated from the specimen by slices of potassium-β-

alumina electrolyte. The voltage was measured between two specially constructured ionic probes described below. These, of course, do not have to be capable of passing a significant ionic current.

Four-point ionic dc measurements on mixed conductors have occasionally found application in studies of silver and copper ion mixed conductors (*1, 8–11*). In these cases the compounds were sufficiently plastic in nature for the parts of the cell to be formed by pressing powders at room temperature, and for contacts to be made simply under mechanical pressure. β Alumina and the ferrites, on the other hand, are hard ceramics and some preliminary experiments had confirmed that good ionic contacts were impossible to make just by pressing together surfaces even when considerable care was taken in machining and polishing. It had been hoped that a good ionically conducting interface between potassium β alumina and potassium ferrite might be made in a single hot-pressing operation, but attempts failed due to cracks at the inter-
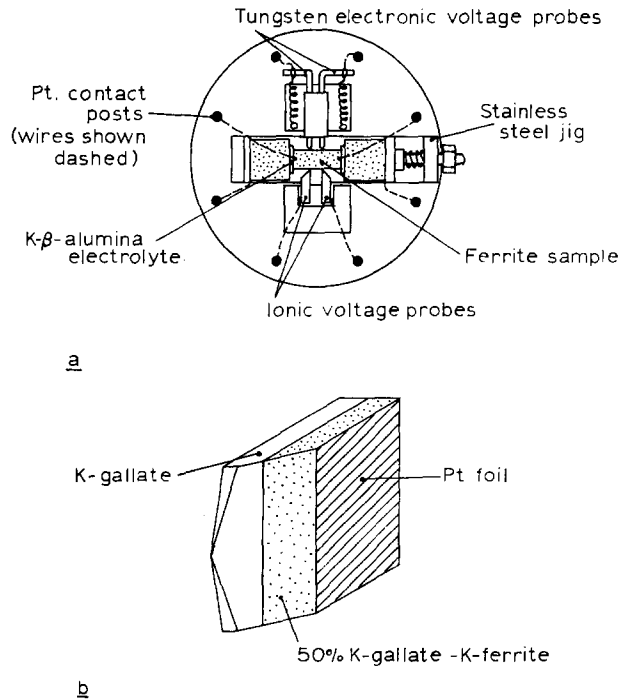

FIG. 1. Experimental arrangement for combined electronic and ionic four-point conductivity measurements. The construction of the ionic voltage probes is shown in (b).

face. Subsequent measurements of thermal expansion coefficients (13) revealed that the value for potassium ferrite was twice that of potassium β alumina (12×10^{-6} compared to 6×10^{-6}). Ionic current contacts were therefore produced by pressing together polished ferrite and β-alumina surfaces, wetted with a trace of molten potassium nitrate.

Experimental Arrangement

This arrangement is shown in Fig. 1. The specimen was in the form of a bar with a 2.7 mm-square cross section and was 5.6-mm long. Each end had a groove cut in it 0.2-mm wide by 0.3-mm deep into which was wedged a length of platinum wire to provide electronic current contacts. The specimen, β alumina slices and ferrite ion reservoirs, were clamped together in a stainless steel jig with a tungsten compression spring. The interface wetting process was carried out in several stages designed to produce a continuous film of potassium nitrate at the interfaces without wetting the sides of the specimen. This consisted of dipping the β-alumina slices into molten potassium nitrate, cooling, assembling the jig, heating it to 670°K (in an inert atmosphere), cooling again, and finally briefly washing in water to dissolve any nitrate adhering to the sides of the bar.

The jig was laid on the alumina-base plate and the sample clamped between the ionic and electronic voltage probes. The construction of the ionic probes is shown enlarged in Fig. 1b. Potassium gallate was used as the electrolyte and 50% gallate ferrite as the electrode because of their thermal expansion compatibility which allowed the interface to be formed by hot pressing preformed slices together with a platinum foil contact. The complete assembly fitted inside a glass envelope in which an argon atmosphere was maintained and this in turn fitted into a resistance furnace. A chromel–alumel thermocouple was placed in contact with the jig.

Measurement Technique

All voltages except that between the ionic probes were measured directly with a high-impedance digital voltmeter. The latter was monitored on the same meter after passing

through a 10^{12}-ohm-input impedance operational amplifier acting as a voltage follower. Currents were supplied by a simple operational amplifier current source and measured by the voltage drop across a standard resistor. A control unit using transistor–transistor logic was built that enabled switching the voltage channel selection to be carried out automatically via reed relays and recorded on a digital printer, according to predetermined programs. A typical sequence of measurements was as follows: the two voltage probe emfs and the thermocouple were monitored for 6000 sec with no current flowing in the specimen in order to establish a base line. A constant current was then switched on and the voltage probes monitored every 10 sec for 400 sec and then at 100-sec intervals. At 12 000 sec the current was switched off, at 18 000 sec it was switched on again in the opposite direction, and at 24 000 sec it was switched off. Typical results are plotted in Figs. 2 and 3. The current was chosen to give a final voltage probe change of 5–10 mV. The composition
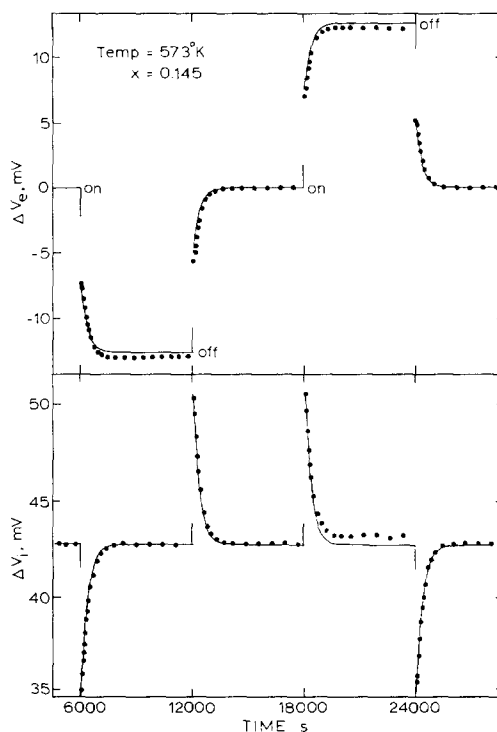

FIG. 2. Voltage probe behavior with time when switching an electronic current on and off.
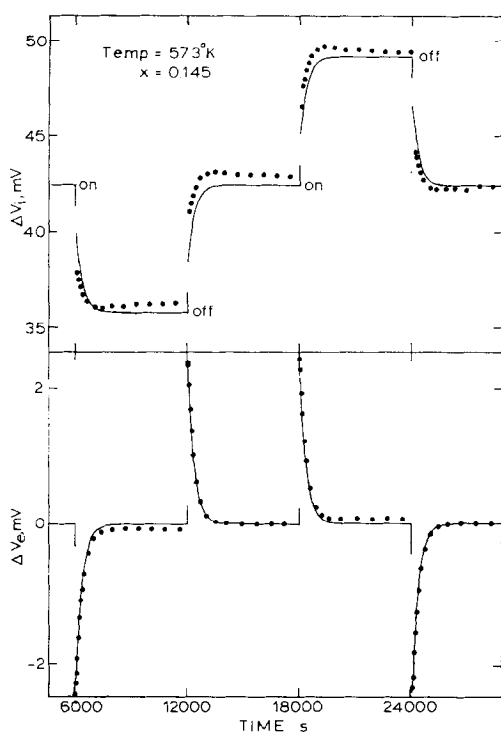
FIG. 3. Voltage probe behavior with time when switching an ionic current on and off.
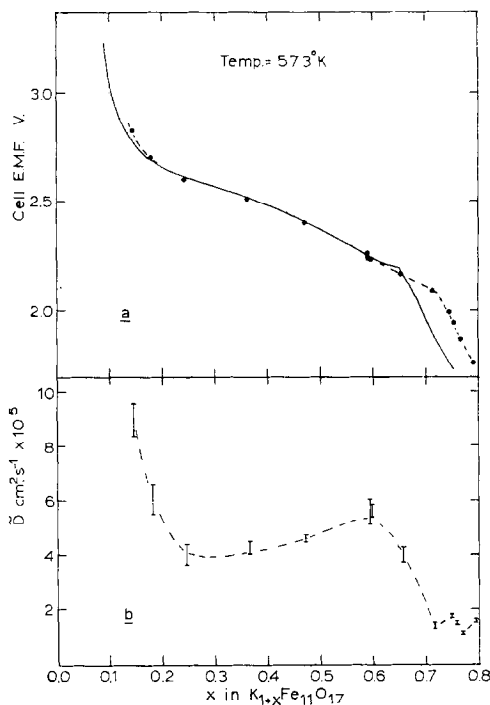

FIG. 4. (a) Equilibrium cell emfs. Results from present work using a K-ferrite-gallate reference electrode (solid circles) have been adjusted to the potassium-metal reference used previously (7); the results are shown by the solid line. (b) The chemical diffusion coefficient $\tilde{D}$ calculated from the transient analysis as a function of x.

of the ferrite specimen was changed *in situ* by passing a constant current between the ion sources and the electronic contacts. One of the ionic voltage probes was used also as reference electrode and its voltage with respect to one of the electronic voltage probes was measured at each composition.

Results and Discussion

Equilibrium Cell emfs

Chemical analysis for potassium on a specimen with the starting composition and the charge passed during the coulometric titrations allowed the value of x in the formula $K_{1+x}Fe_{11}O_{17}$ to be calculated for each composition studied. The potassium activity in the sample was referenced to that in 50% ferrite gallate, and not to metallic potassium, so that a direct comparison with the titration curve reported previously (7) was not possible. However, adjustment of the voltage axis origin allowed a moderate fit to be obtained as

shown in Fig. 4. The limitations of the accuracy of the analysis (flame emission analysis of a 30-mg sample dissolved in HCl) leaves an uncertainty of about ±0.04 in the position of the origin of the x axis, so that it is not possible to decide with certainty whether the movement of the "shoulder" of the E versus x curve is significant. The interval in x between this and the region where the emf becomes asymptotic to the vertical is nevertheless slightly larger.

Electronic and Ionic Conductivities—Steady-State Conditions

The potassium metal concentration in potassium ferrite would be expected to be vanishingly small in view of its very low activity. The iron–oxygen framework is also expected to be essentially immobile at the temperatures concerned here. Thus only the carriers K^+ and

e^- will be considered in the analysis of the transport properties. If z is the flux direction (along the axis of the bar) the isothermal flux equations in terms of particle quantities can be written:

$$-\frac{j_i}{e} = L_{ii}\frac{\partial\bar{\mu}_i}{\partial z} + L_{ie}\frac{\partial\bar{\mu}_e}{\partial z}. \qquad (1)$$

$$\frac{j_e}{e} = L_{ei}\frac{\partial\bar{\mu}_i}{\partial z} + L_{ee}\frac{\partial\bar{\mu}_e}{\partial z}. \qquad (2)$$

where j is a current density, $\bar{\mu}$ a particle electrochemical potential, e the electronic charge, and L the general Onsager phenomenological coefficient. Subscripts i and e refer to potassium ions and electrons, respectively.

Since no current flows within the voltage probes these provide one with a direct measure of the electrochemical potential of the species to which they are reversible at the point of contact with the bar. Thus considering the potential differences ΔV_i and ΔV_e between these probes:

$$\Delta V_i = \Delta\bar{\mu}_i/e + \text{const}; \qquad \Delta V_e = \Delta\bar{\mu}_e/e. \quad (3)$$

The constant in the ionic probe expression arises from the fact that the two potassium reference materials (nominally 50% K ferrite–K gallate) do not in general have exactly the same potassium activity. When an ionic current density j_i is passed through the bar and a steady state has been set up j_e must be everywhere zero. Together with the Onsager relation $L_{ie} = L_{ei}$ one obtains from Eq. (2):

$$\frac{\partial\bar{\mu}_e}{\partial z} = \frac{-L_{ie}}{L_{ee}}\frac{\partial\bar{\mu}_i}{\partial z}. \qquad (4)$$

Then Eq. (1) becomes:

$$-j_i/e = \left(L_{ii} - \frac{L_{ie}^2}{L_{ee}}\right)\frac{\partial\bar{\mu}_i}{\partial z}. \qquad (5)$$

The ionic conductivity measured (σ_i') is given by:

$$\sigma_i' = \frac{j_i\,\Delta z_i}{\Delta V_i}, \qquad (6)$$

where Δz_i is the distance between the ionic voltage probes. Taking Eqs. (3) and (6) and provided that the L coefficients are independent of $\bar{\mu}_i$, Eq. (5) becomes:

$$\sigma_i' = e^2\left(L_{ii} - \frac{L_{ie}^2}{L_{ee}}\right). \qquad (7)$$

Here the superscript is used in accordance with Wagner (12) who recently pointed out the difference between this conductivity for suppressed transport of electrons where a concentration gradient is set up along the bar and the "partial" ionic conductivity σ_i obtained in the absence of concentration gradients, for example by combining transport number determinations with the total conductivity. He showed that they would only be the same in the case that $L_{ie} = 0$, for which the flux equations reduce to the ideal form in which there is no coupling between the two fluxes. Although no significant "chemical" association of potassium ions and electrons is to be expected in the present case the very large concentrations of the two species compared to those met in traditional defect chemistry leaves the possibility of long-range coulombic interactions leading to nonzero values of L_{ie}. From Eqs. (3) and (4) it can be seen that the ratios L_{ie}/L_{ii} and L_{ie}/L_{ee} can be simply obtained from the ratio of the steady-state probe voltages:

$$(\Delta V_e/\Delta z_e)/(\Delta V_i/\Delta z_i)_{\substack{j_e=0. \\ \text{steady} \\ \text{state}}} = -\frac{L_{ie}}{L_{ee}};$$

$$(\Delta V_i/\Delta z_i)/(\Delta V_e/\Delta z_e)_{\substack{j_i=0. \\ \text{steady} \\ \text{state}}} = -\frac{L_{ie}}{L_{ii}}. \quad (8)$$

The behavior of the two sets of voltage probes with time on passing an electronic current is shown for a typical experiment by the points in Fig. 2, and in the case of an ionic current in Fig. 3. It is immediately apparent that in both cases the voltage probes reversible to the blocked carriers returned closely to their voltage before any current was passed. L_{ie}/L_{ii} was calculated for all experiments. For $x > 0.4$ the uncertainty in the ionic probe voltage due to noise and stray emfs allows only an upper limit of ±0.04 to be obtained. At lower x values L_{ie}/L_{ii} was definitely positive and in the range 0.02–0.08. We therefore conclude that the coupling between the fluxes is very small. One might speculate that this is due to the electrons being essentially contained in the spinel block portions of the crystal structure, while the mobile potassium ions are constrained within the mirror planes, thus

reducing the opportunity for interaction. The only other measurements of this type known to the authors are those reported by Yokota (1) for silver telluride with the stoichiometry $Ag_{1.98}Te$. Although the possibility of coupling of the fluxes of silver ions and electronic carriers was not considered the probe behavior reported again indicates a very small value of L_{ie}/L_{ii}. This is somewhat more surprising since both direct chemical association and coulombic coupling might be expected to be much easier in this system.

In what follows L_{ie} has been effectively neglected. The conductivities σ'_i and σ'_e are now identified with the partial conductivities σ_i and σ_e and the flux equations reduce to the usual form for independently moving carriers, which in terms of conductivities read:

$$- j_i = (\sigma_i/e)(\partial \bar{\mu}_i/\partial z); \qquad j_e = (\sigma_e/e)(\partial \bar{\mu}_e/\partial z).$$
$$(9)$$

The condition of local equilibrium, $K \rightleftharpoons K^+ + e^-$, demands that the relation $\bar{\mu}_i + \bar{\mu}_e = \mu$ must hold, where μ is the chemical potential of potassium (metal), and with $j_e = 0$ one obtains:

$$- j_i = (\sigma_i/e)(\partial \mu_i/\partial z) = (\sigma_i/e)(\partial \mu/\partial z). \quad (10)$$

The ionic electrochemical potential gradient is seen to be identical to the gradient of the chemical potential of potassium down the bar. The value of σ measured is thus an average value between those corresponding to compositions at the two voltage probes. It is consequently necessary to work with very small currents.

Instantaneous Probe Voltages on Switching on the Current

At the instant of turning on the current both carriers are free to move and the bar has a uniform composition. Expanding Eqs. (1) and (2) one has:

$$-j_i = L_{ii}\left(\frac{\partial \mu_i}{e\partial z} + \frac{\partial \phi}{\partial z}\right) + L_{ie}\left(\frac{\partial \mu_e}{e\partial z} + \frac{\partial \phi}{\partial z}\right). \quad (11)$$

$$j_e = L_{ei}\left(\frac{\partial \mu_i}{e\partial z} + \frac{\partial \phi}{\partial z}\right) + L_{ee}\left(\frac{\partial \mu_e}{e\partial z} + \frac{\partial \phi}{\partial z}\right). \quad (12)$$

Under these conditions all chemical potential gradient terms vanish and consequently both sets of voltage probes should give the *same* voltage gradient: $(\Delta V/\Delta z)$ given by:

$$\frac{\Delta V}{\Delta z} = \frac{\Delta \phi}{\Delta z}. \quad (13)$$

Furthermore the conductivity calculated from: $\frac{j\Delta z}{\Delta V}$ is the total conductivity $(\sigma_i + \sigma_e)$. In this work the voltage so measured conformed to this within experimental error *except* for the case of the ionic probe voltage on switching on an ionic current. In this case the switch-on voltage was generally too large and sometimes fell for a short period before increasing again to the steady-state value. The reason for this is uncertain but may be associated with stray capacitances in the measuring system.

Probe Behavior Before a Steady State Is Reached

The time taken for the steady-state voltage conditions to be reached was typically about 1 hr. Similar transient effects, although of shorter duration have previously been reported by Roth and Romanczuk (5) Takahashi (6), and by the present authors (7) in the potassium ferrite system. Roth interpreted them in terms of a simple equivalent circuit consisting of electronic and ionic resistances in parallel, with a capacitor in series with the ionic resistor to represent the effects of the ion-blocking electrodes. The application or removal of a constant current to this circuit leads to exponential rises and decays in the emfs of both types of voltage probe with a characteristic time constant T given by:

$$T = (R_e + R_i)C. \quad (14)$$

Yokota (1) has, however, calculated the expected transient response of voltage probes in a mixed conductor, assuming zero cross coefficients, and shown that the results agreed with the experiment in the case of silver telluride. He showed that provided σ_i, σ_e and $d\mu/dN$, (the variation of metal activity with concentration) could be regarded as constant over the composition range along the con-

ductivity specimen, the problem reduced to that of simple diffusion:

$$\frac{\partial N}{\partial t} = D \frac{\partial^2 N}{\partial z^2},$$

where:

$$D = \frac{\sigma_i \sigma_e}{(\sigma_i + \sigma_e) e^2} \left(\frac{d\mu}{dN}\right). \qquad (15)$$

It can be shown that D is simply the chemical or mutual diffusion coefficient $\tilde{D}$ for the system (14). In calculating the time dependence of the voltage probe emfs he took account of a linear variation of σ_e upon N, while assuming that σ_i was essentially independent of composition. In the case of potassium ferrite preliminary results confirmed that both σ_i and σ_e can be regarded as constant over the small composition range corresponding to cell emf ranges of ± 10 mV, and thus the small current approximations given by Yokota should be adequate.

In potassium ferrite the molar concentration of electronic carriers is equal to $x - \mathrm{const}$ where the constant corresponds to the composition at which the observed electronic conductivity falls to zero (7). The concentration of potassium ions is equal to $1 + x$. Thus the value of $d\mu/dN$ can be obtained in terms of molar quantities as follows:

$$\frac{d\mu}{dN} = \frac{\partial x}{\partial N} \cdot \frac{\partial \mu}{\partial x} = \frac{M}{\rho (N_0)^2} F \frac{\partial E}{\partial x}, \qquad (16)$$

where E is the emf corresponding to the activity of potassium (metal) in the sample with respect to a suitable reference, M the molecular weight, and ρ the density of the ferrite. N_0 is Avogadro's number and F the Faraday. Yokota obtained the following expressions for the individual probe voltages. For switching on an ionic current:

$$V_i = -\frac{jZ}{\sigma_i} \left\{ \frac{z}{Z} - \frac{1}{2} + \left(\frac{\sigma_e}{\sigma_e + \sigma_i}\right) \phi \left(\frac{z}{Z}, \frac{t}{\tau}\right) \right\}, \qquad (17)$$

where Z is the length of the bar specimen and z the distance of the probe from the end

$$V_e = \frac{jZ}{(\sigma_i + \sigma_e)} \phi \left(\frac{z}{Z}, \frac{t}{\tau}\right). \qquad (18)$$

After switching off the current:

$$V_i = \frac{jZ}{(\sigma_i + \sigma_e)} \frac{\sigma_e}{\sigma_i} \phi \left(\frac{z}{Z}, \frac{t}{\tau}\right), \qquad (19)$$

and:

$$V_e = \frac{-jZ}{(\sigma_i + \sigma_e)} \phi \left(\frac{z}{Z}, \frac{t}{\tau}\right), \qquad (20)$$

The function $\phi(\xi, s)$ is given by:

$$\phi(\xi, s) = \frac{4}{\pi^2} \sum_{m=0}^{\infty} \frac{1}{(2m + 1)^2}$$
$$\times \exp[-(2m + 1)^2 s] \cos[(2m + 1)\pi\xi]. \qquad (21)$$

and

$$\frac{1}{\tau} = \tilde{D} \frac{\pi^2}{Z^2} = \frac{\pi^2 \sigma_i \sigma_e M}{Z^2 (\sigma_i + \sigma_e) F \rho} \frac{dE}{dx}. \qquad (22)$$

The relation:

$$\phi \left(\frac{z}{Z}, \frac{t}{\tau}\right) = -\phi \left(\frac{Z - z}{Z}, \frac{\tau}{t}\right).$$

holds so that when the voltage probes are spaced symmetrically about the center of the bar, Eqs. (17)–(20) become, respectively:

$$\Delta V_i - \Delta V_{i,\infty} = \frac{-2jZ\sigma_e}{(\sigma_e + \sigma_i)\sigma_i} \phi \left(\frac{Z - \Delta z}{2Z}, \frac{t}{\tau}\right). \qquad (23)$$

$$\Delta V_e - \Delta V_{e,\infty} = \frac{+2jZ}{(\sigma_e + \sigma_i)} \phi \left(\frac{Z - \Delta z}{2Z}, \frac{t}{\tau}\right). \qquad (24)$$

$$\Delta V_i - \Delta V_{i,\infty} = \frac{+2jZ\sigma_e}{(\sigma_e + \sigma_i)\sigma_i} \phi \left(\frac{Z - \Delta z}{2Z}, \frac{t}{\tau}\right). \qquad (25)$$

$$\Delta V_e - \Delta V_{e,\infty} = \frac{-2jZ}{(\sigma_i + \sigma_e)} \phi \left(\frac{Z - \Delta z}{2Z}, \frac{t}{\tau}\right). \qquad (26)$$

where ΔV_∞ is the probe voltage difference at $t = \infty$.

Interchanging subscripts gives the corresponding relations for electronic currents. It can be shown that for t/τ greater than 0.3 all terms of $\phi(\xi, s)$ other than the first become negligible and $\phi(\xi, s) \sim (4/\pi^2) \exp - t/\tau \cos \pi\xi$ and the probe voltage relations reduce to the form given by the simple equivalent circuit. Identifying T in Eq. (14) with τ and putting $R_e = (Z/\sigma_e A)$ and $R_i = (Z/\sigma_i A)$ where A is the

area of cross section of the specimen it can be shown that:

$$C = \frac{AZ}{\pi^2} \frac{F\rho}{M \, dE/dx}.$$ (27)

C would be expected to be relatively independent of temperature as found by Roth (5).

Using σ_i and σ_e values from steady emfs and (dE/dx) from the E vs x graph (Fig. 4a) the theoretical curves for the run shown in Figs. 2 and 3 were computed (solid lines). The fit is on the whole quite good. The deviation from exponential behavior predicted by Yokota for small times is also visible.

For all experiments τ was calculated from the slope of plots of log $|\Delta V - \Delta V_\infty|$ versus time, neglecting short times. Typical results are shown in Fig. 5. τ values for all combinations of currents and probes as well as switching on and off agreed to within 10–20% which was considered satisfactory in view of the significant scatter in the voltage readings; especially those of the ionic probes where the voltages were only a few millivolts from a source impedence of some 10^7 ohm. The values
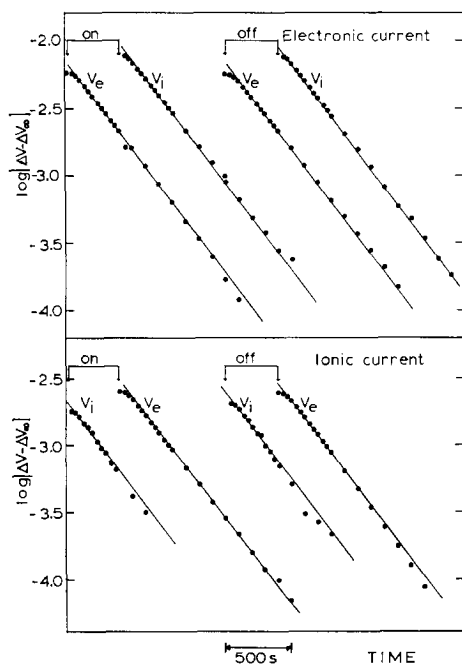

FIG. 5. Log $|\Delta V - \Delta V_\infty|$ versus time for both sets of voltage probes on switching on and off (a) electronic and (b) ionic currents.

of D obtained from τ are shown in Fig. 4b as a function of x.

Ionic Conductivity Results

Values of σ_i obtained from the steady-state conditions (Eq. (6)) are shown as solid circles in Fig. 6 as a function of x. σ_i could also be calculated independently from the transient analysis using measured values of t, σ_e, and (dE/dx), in Eq. (22). These are shown as open circles in Fig. 6. At low x values (dE/dx), became difficult to measure accurately and another alternative independent calculation of σ_i was used employing measured values of $(\sigma_i + \sigma_e)$ from the instantaneous switch-on conditions and σ_e. These are shown by crosses in Fig. 6.

The technique of promoting a good ionic contact by wetting interfaces with potassium nitrate proved not entirely satisfactory. At 300°C the film was presumably solid although it conducted sufficiently for the required current to be passed using an ionic current electrode driving voltage of about 500 mV. However after 4 weeks of operation the contact gradually deteriorated and the ionic probe behavior as a function of time began to change. Eventually it became impossible to obtain a reliable steady-state ionic probe emf and the values of σ_i estimated were much smaller than those obtained at corresponding compositions at an earlier stage. However the electronic probes continued to respond normally during ionic current experiments. Furthermore both probes behaved normally during electronic current runs. The problem was therefore attributed to an uneven and time-variable contact at the ionic current probes, leading to a nonhomogeneous flux along the bar. The interface was reassembled twice during the course of the measurements, but the fact that the steady-state ionic conductivities tend to be some 10–50% below the values obtained from the transients may reflect the difficulties with the interface, although the former values would normally be expected to be more accurate.

Activation Energy for Ionic Conduction

Conductivity experiments were carried out as a function of temperature for the composi-
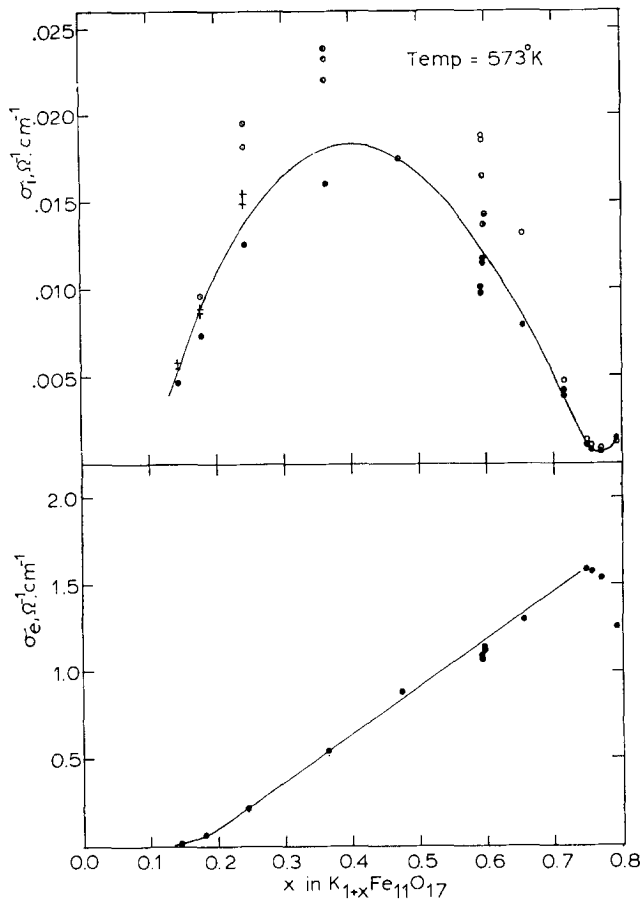
FIG. 6. Ionic conductivity σ_i and electronic conductivity σ_e of potassium ferrite as a function of the potassium ion excess x.

tion $x = 0.60$. Log σ_i and log σ_e are shown versus $1000/T$ in Fig. 7. The ionic conductivity was described by the equation $\sigma_i = 2.236 \exp (-Ea/RT)$ with $Ea = 25.0 \pm 2.5$ kJ/mole in good agreement with the value of 25.5 ± 4.2 found by Roth and Romanczuk (5). Since the ionic transport number at this composition is less that 0.01, Eq. (22) can be approximated by:

$$\tilde{D} = \frac{\sigma_i M}{F} \frac{dE}{dX}. \qquad (28)$$

The activation energy for chemical diffusion will be the same as for ionic conduction provided (dE/dX) is not strongly temperature sensitive. Thus we obtain

$$\tilde{D} = 6.56 \times 10^{-3} \exp \frac{-25.0 \times 10^3}{RT}.$$

Hever (4) obtained for the potassium ion tracer diffusion coefficient in a mixed potassium–sodium ferrite:

$$D^* = 1.05 \times 10^{-3} \exp \frac{-30.14 \times 10^3}{RT}.$$

Apart from correlation effects which could lower the value of the preexponential factor, the higher activation energy might be ascribed to a decrease in the conduction plane slot width on partial substitution of sodium for potassium.

Electronic Conductivity

The electronic conductivity measurements, shown in Fig. 6 follow the same trends as previously reported (7). However they are smaller by a factor of 2.7. This is probably
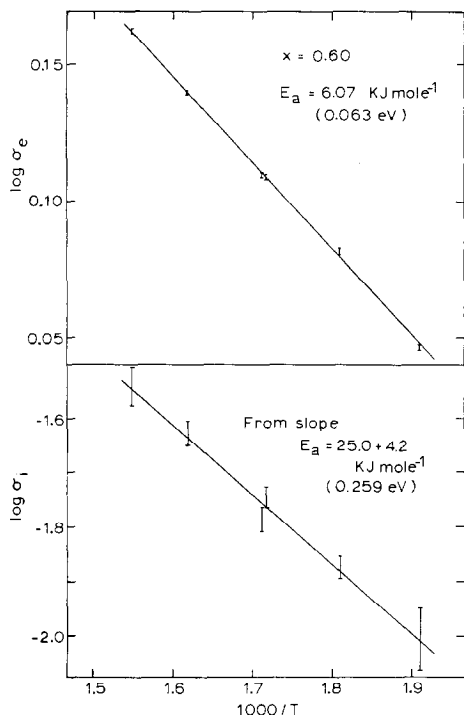
FIG. 7. Log σ_i and log σ_e versus reciprocal temperature at the composition $x = 0.60$.

attributable to differences in the microstructure between the two samples. In particular the observed tendency for crystallites to orient themselves during hot pressing would have dramatic effects on the measured conductivities because of the two-dimensional conduction process. The samples in both sets of measurements were cut from hot pressed pellets in a way that would be expected to give the highest conductivity values, i.e., in the present work with the bar axis perpendicular to the hot pressing axis. The activation energy was 0.063 eV for electronic conduction at $x = 0.60$, in close agreement to that found previously (7). It is not known whether the drop in σ_e at very high x values is significant or whether it is associated with hysteresis effects noticed in Part I (7).

The Thermodynamics of Dissolution of Potassium in Potassium Ferrite

In a previous paper (7) the authors reported measurements of cell emfs as a function of x at 250°C using potassium metal as the refer-

ence potassium activity. The cell emf was also monitored as a function of temperature over the range 150–350°C, allowing the partial enthalpy and entropy changes on dissolution of potassium in the ferrite phase to be calculated from the relations: $\Delta S = F(\partial E/\partial T)$; $\Delta H = F((T\partial E/\partial T) - E)$. The results are shown in Fig. 8. Experimental details were reported previously (7). The sudden change of slope at $x = 0.65$ in the cell emf versus x curve (Fig. 4) is accompanied by a deep minimum in the entropy of solution suggesting that some sort of ordering process is occurring at this composition. For $x > 0.65$, the previously relatively constant enthalpy starts to fall rapidly showing that the addition of more potassium atoms is becoming much more energetically unfavorable. A similar, but much smaller effect may also be occurring around $x = 0.12$, while at $x = 0.2$ the small minimum in ΔH indicates that a separation into two phases may occur in this composition region at sufficiently low temperatures.
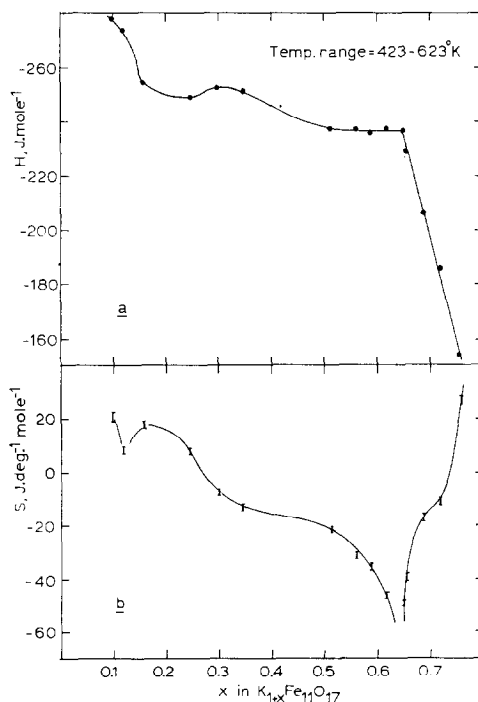

FIG. 8. (a) Enthalpy and (b) entropy of dissolution of potassium in potassium ferrite as a function of composition.

A recent determination of the phase diagram of the $KFeO_2$–Fe_2O_3 system (15) shows the region of nonstoichiometry of two-block K-ferrite as extending from $K_2O \cdot 6Fe_2O_3$ to $K_2O \cdot 6.8Fe_2O_3$. This corresponds to the region of x values between 0.62 and 0.83. That the ordered composition is within this range may prove significant.

Comparison of Results with Theoretical Models for Ionic Conduction in β-Alumina

Figure 9a shows a section through the unit cell of β alumina in the alkali-ion conduction plane. The crystal lattice energy calculations by Wang, Gaffari, and Choi (2) show that the Beevers–Ross sites for alkali ions represent deep potential wells and consequently any ions in these positions are not very mobile.

Alkali ion sites:
BR Beevers-Ross sites
ABR Anti-BR sites   Shaded circles are
MO Mid-Oxygen sites   bridging $O^=$ ions

a

● BR sites   o ABR sites   • MO sites

b

FIG. 9. (a) Section through the conduction plane of the β-alumina structure showing possible sites for the mobile ions. (b) Hexagonal conduction path network formed by joining the alkali ion sites of adjacent unit cells. Unit cell boundaries are shown as dotted.

On the other hand when an excess x of alkali ions per unit cell mirror plane are present, energetic considerations lead to the prediction that $2x$ ions will take up mid-oxygen sites, midway between the Beevers–Ross and anti-Beevers–Ross sites leaving $1 - x$ in Beevers–Ross positions. These mid-oxygen alkali ions are expected to be responsible for ionic conductivity via an interstitialcy mechanism. For very low x values therefore, one would expect that σ_i would be proportional to x. For higher x values the availability of vacant adjacent interstitial sites becomes important and one would expect to get a relation of the form:

$$\sigma_i \propto x(1 - x). \qquad (29)$$

This simple expression predicts the same parabolic dependence of the conductivity upon concentration as reported previously for oxide fluorite solid solutions (17) but does not take into account the effect of ion–ion interactions about which little is known at present.

Sato and Kikuchi (16) have used the path probability method to calculate the effects of ion–ion interactions on σ_i and D_i^*. However their model is rather different in that Beevers–Ross, and anti-Beevers–Ross sites are considered as the stable alkali ion rest positions. The low-temperature distribution is assumed to be a full occupation of the Beevers–Ross sites with the excess x ions occupying anti-Beevers–Ross sites. Although all three types of site lie on the same "honeycomb" conduction network, shown in Fig. 9b, it would be expected that considerable differences would exist in the analysis of the two models, particularly at relatively high x values where in Wang's model a larger number of sites will still be vacant and the possibility of further ordering effects among the mid-oxygen sites might occur.

The fall in σ_i at low x values strongly supports Wang's conclusion that ions in Beevers–Ross sites are relatively immobile. Furthermore, the parabolic law of Eq. (29) is clearly present, although the maximum is at $x \sim 0.35$ rather than 0.5. Nevertheless, a similar behavior can be obtained from Sato and Kikuchi's calculations if a suitable value of the temperature parameter is chosen. The
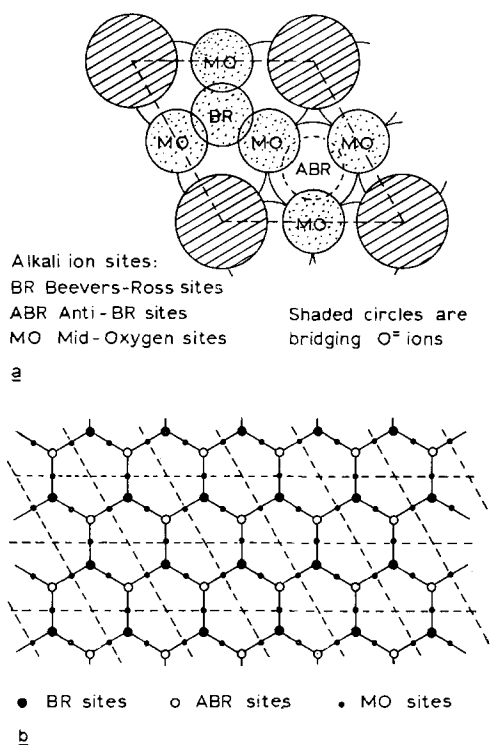
observed shift in the σ_i maximum to lower x values is opposite to that predicted in the case of repulsive ion–ion interactions favored by Sato and Kikuchi but is most likely in this case to be due to the onset of a potassium ion ordering process strongly indicated by the entropy data. The discontinuity in the diffusion coefficient around $x = 0.7$ can also be explained by the sudden increase in the thermodynamic factor dE/dX at this composition. Work is in progress to obtain direct structural confirmation of the ordering process. Le Cars et al. (18) have reported ordering of silver ions in silver β alumina with stoichiometry close to $Na_{1.33}Al_{11}O_{17}$ and show that a related ordering arrangement would be possible at $x = 0.66$. Ordering was only observed at low temperatures, however.

In conclusion, potassium ferrite has proved a useful model for studying the ionic conduction process in β-alumina-type compounds. Fortunately the very small coupling between electronic and ionic fluxes indicates that the ionic conduction process should be directly comparable to that in electrolyte materials and not affected seriously by electronic conductivity. The conduction process is a complicated one involving a variety of jump frequencies and barrier heights as shown by microwave and NMR investigations on β alumina (19). At present models are not available which take into account such complicating factors as the presence of extra interstitial oxygen ions in the conduction plane (20).

Acknowledgment

References

1. J. YOKOTA, J. Phys. Soc. Japan 16, 2213 (1961).
2. J. C. WANG, M. GAFFARI, and S. CHOI, J. Chem. Phys. 63, 772 (1975).
3. B. C. H. STEELE, in "Superionic Conductors" (G. D. Mahon and W. L. Roth, Eds.), New York, Plenum Press, 1976.
4. K. O. HEVER, J. Electrochem. Soc. 115, 826, 830 (1968).
5. W. L. ROTH and R. J. ROMANCZUK, J. Electrochem. Soc. 116, 975 (1969).
6. T. TAKAHASHI, K. KUWABARA, AND Y. KASE, Nippon Kagaku Kaishi, 1305 (1975).
7. G. J. DUDLEY, B. C. H. STEELE, AND A. T. HOWE, J. Solid State Chem. 18, 141 (1976).
8. H. RICKERT, Z. Phys. Chem. N.F. 23, 355 (1960).
9. N. VALVERDE, Z. Phys. Chem. N.F. 70, 128 (1970).
10. T. TAKAHASHI, O. YAMAMOTO, F. MATSUYAMA, AND Y. NODA, J. Solid State Chem. 16, 35 (1976).
11. T. TAKAHASHI AND O. YAMAMOTO, J. Electrochem. Soc. 119, 1735 (1972).
12. C. WAGNER, Progr. Solid State Chemistry 10, 3 (1975).
13. G. J. DUDLEY AND B. C. H. STEELE, to appear.
14. L. HEYNE, Mass Transport in Oxides N.B.S., Special Publication 296 (Washington, U.S. Government Printing Office 1968).
15. T. TAKAHASHI, K. KUWABARA, AND Y. KASE, Denki Kagaku 43, 273 (1975).
16. H. SATO AND R. KIKUCHI, J. Chem. Phys. 55, 677 (1971).
17. B. C. H. STEELE AND C. B. ALCOCK, Trans. A.I.M.E. 233, 1359 (1965).
18. Y. LeCARS, R. COMÈS, L. DESCHAMPS, AND J. THERY, Acta Crystallogr. A30, 305 (1974).
19. S. J. ALLEN JR., L. C. FELDMAN, D. B. McWHAN, J. P. REMEIKA, AND R. E. WALSTEDT, in "Superionic Conductors" (G. D. Mahon and W. L. Roth, Eds.), New York, Plenum Press, 1976.
20. W. L. ROTH, General Electrical Research Report 74, CRD054 (1974).